○ Geoscience Letters

RESEARCH LETTER

Open Access

CMIP6 model-based analog forecasting for the seasonal prediction of sea surface temperature in the offshore area of China

Weiying Peng[1,2], Quanliang Chen[1], Shijie Zhou[2] and Ping Huang[2,3*] ⓘ

Abstract

Seasonal forecasts at lead times of 1–12 months for sea surface temperature (SST) anomalies (SSTAs) in the offshore area of China are a considerable challenge for climate prediction in China. Previous research suggests that a model-based analog forecasting (MAF) method based on the simulations of coupled global climate models provide skillful climate forecasts of tropical Indo-Pacific SSTAs. This MAF method selects the model-simulated cases close to the observed initial state as a model-analog ensemble, and then uses the subsequent evolution of the SSTA to generate the forecasts. In this study, the MAF method is applied to the offshore area of China (0°–45°N, 105°–135°E) based on the simulations of 23 models from phase 6 of the Coupled Model Intercomparison Project (CMIP6) for the period 1981–2010. By optimizing the key factors in the MAF method, we suggest that the optimal initial field for the analog criteria should be concentrated in the western North Pacific. The multi-model ensemble of the optimized MAF prediction using these 23 CMIP6 models shows anomaly correlation coefficients exceeding 0.6 at the 3-month lead time, which is much improved relative to previous SST-initialized hindcasts and appears practical for operational forecasting.

Keywords: Seasonal forecasts, Model-based analog forecasting, CMIP6, Offshore area of China

Introduction

The offshore area of China (0°–45°N, 105°–135°E), including the Yellow Sea (33°–39°N, 120°–128°E) and Bohai Sea (37°–41°N, 117°–122°E) (YBS), East China Sea (ECS; 23°–34°N, 117°–131°E) and South China Sea (SCS; 2°–22°N, 105°–120°E), stretches from the tropics to the subtropics with a large temperature span (Cai et al. 2011). As one of the largest areas of ocean–land convergence, the offshore area of China has a unique marine environment with a wide range of sea areas, a long coastline, and numerous coastal harbors and estuaries, with a fundamental impact on marine ecology (Cai et al. 2006, 2011; Tan et al. 2016). Besides, the oceanic environment in the offshore area of China is closely interrelated with the East Asian–western North Pacific climate (Lin et al. 2005). Therefore, an accurate short-term climate forecast for the oceanic environment, such as the sea surface temperature (SST), in the offshore area of China is of great importance (Liu et al. 2018; Qi and Cai 2019; Song et al. 2016; Wang et al. 2020b; Wei et al. 2020).

At present, the seasonal forecasting of SST mainly depends on the initialization prediction of dynamic models. For instance, researchers utilize the hindcasts and real-time predictions from multi-model ensemble system, initialization parameter ensemble, and coupled general circulation models (Barnston et al. 2019; Keenlyside et al. 2016; Merryfield et al. 2013). However, dynamic models often have inevitable defects that limit their prediction skill in some areas. In particular, the skill of SST seasonal forecasts in the offshore area of China produced by dynamic models is quite low, possibly due

*Correspondence: huangping@mail.iap.ac.cn
[2] Center for Monsoon System Research, Institute of Atmospheric Physics, Chinese Academy of Sciences, Beijing, China
Full list of author information is available at the end of the article

to the complex ocean–land boundary around this region (Li et al. 2005; Ren et al. 2015; Wang et al. 2004). However, the most common climate models cannot be easily adjusted for a particular area. Thus, there is a great challenge to improve the prediction skill for SST in the offshore area of China.

The analog forecasting method which based on observation data has a long history in weather forecasting (Toth 1987; Van den Dool 1989). Recently, a model-based analog forecasting (MAF) method has been developed, researchers apply dynamic model analogue correction scheme to improve the short-term and long-term precipitation forecasting (Gong et al. 2016; Singh and Kumar 2020) and applied the MAF in the prediction of tropical SST (Ding et al. 2018, 2019; Wang et al. 2020a). The MAF method utilizes long-term control runs of climate models as library datasets, and further selects cases from the library datasets to generate predictions. The selected cases are analogous to the initial values determined by some metrics. Because MAF can use the model simulations executed beforehand, this method can greatly save on prediction costs compared with initialized dynamic prediction. Ding et al. (2018) showed that the MAF method can achieve similar skill to the initialized prediction of the North American Multimodel Ensemble for the Indo-Pacific SST anomaly (SSTA). Wang et al. (2020a) further optimized the algorithm and variables in the analog criterion for case selection, and obtained a much-improved prediction skill for the Indo-Pacific SSTA, which was even better than the initialized dynamic prediction by the same model. These results imply a high capacity of the MAF method in short-term SSTA prediction.

Although the anomaly correlation coefficient (ACC) of the improved MAF method at a 3-month lead time in Wang et al. (2020a) was also improved over the offshore area of China relative to the previous SST-initialized hindcast, the ACC value of nearly 0.35 at this lead time is not practical for operational forecasting. However, all the parameters of the MAF method in Wang et al. (2020a) were optimized for predicting the Indo-Pacific SSTA, and thus some key parameters should be further optimized for new applications. Moreover, the Coupled Model Intercomparison Project (CMIP) has released a vast amount of datasets, including pre-industrial control (piControl) simulations longer than 500 years (Eyring et al. 2016). These datasets provide a wealth of resources for applying the MAF method in short-term SSTA prediction.

In this paper, we apply the MAF method to short-term SSTA prediction in the offshore area of China based on the piControl runs of 23 models participating in phase 6 of CMIP (CMIP6). Some optimizing factors, including the area of the initial field and predictor, are investigated to improve the prediction skill.

Methods and datasets
Model-based analog
The MAF method first defines a metric to measure the distance/similarity between the observation cases and model library. Here, the root-mean-square (RMS) is used as the metric to measure the distance between the observation state $x(t)$ and model library state $y(t')$ at each initialization time, t and t' are the initialization time of the observation state and the initialization time of the library state, respectively. The distance metric can be expressed as Ding et al. (2018):

$$d^2(t, t') = \sum_{i=1}^{I} \sum_{j=1}^{J} \left(\frac{x_j^i(t)}{\sigma_X^i} - \frac{y_j^i(t')}{\sigma_Y^i} \right)^2, \quad (1)$$

where i and j are the predictor variables and gridpoint index, I and J represent the number of predictor variables and grid points, and σ_X^i and σ_Y^i are the area-averaged standard deviation of the initial field for the analog criteria with respect to each predictor variable. Then, the distances are sorted in ascending order, and the top N states closest to the observation state are selected into the analog ensemble, while the optimal range of the analog ensemble members N is 50–60 (Wang et al. 2020a). In this study, $N = 60$ is used as the number of analog ensemble members. For each model, the subsequent τ months' evolution of the analog ensemble mean represents the ensemble forecast at the lead time of τ months of the MAF. The multi-model ensemble mean (MME) forecast is the average of the forecast ensemble of all models. Following previous research (Ding et al. 2018, 2019; Wang et al. 2020a), we use the SSTA and sea surface height anomaly (SSHA) as the primary predictor variables.

Data
The piControl runs of 23 CMIP6 models are used as the library datasets in the MAF method. In the piControl run, the CO_2 concentration is maintained at the level before the industrial revolution (Eyring et al. 2016). For each CMIP6 model, the piControl simulation is used as its library data. The library lengths of the models are shown in Table 1. Due to the lack or incompleteness of sea-ice data in some models, only 19 CMIP6 models are selected when Arctic sea-ice anomaly (ASIA) is used as the predictor variable. The observation data for the initial states in the MAF method are obtained from the SST and Arctic sea ice from Met Office Hadley Centre's sea ice and sea surface temperature dataset (HadISST) (Rayner et al. 2003), and the sea surface height (SSH) form the Simple Ocean Data Assimilation (SODA) (Carton and

Peng *et al. Geosci. Lett.* (2021) 8:8

Page 3 of 8

Table 1 Names and library lengths of 23 CMIP6 models

Model name	Library length (years)
BCC-CSM2-MR	600
BCC-ESM1	451
CAMS-CSM1-0*	500
CanESM5	1000
CESM2-WACCM	400
CESM2	1101
CNRM-CM6-1-h	300
CNRM-CM6-1*	500
CNRM-ESM2-1	500
E3SM-1–0	500
EC-Earth3-Veg	500
EC-Earth3	501
FGOALS-f3-L*	500
GFDL-CM4	500
GISS-E2-1-H	801
HadGEM3-GC31-LL	500
IPSL-CM6A-LR*	1200
MIROC-ES2L	500
MIROC6	800
MPI-ESM1-2-h	500
NESM3	500
NorCPM1	500
SAM0-UNICON	700

Models marked with an asterisk (*) do not have an output of Arctic sea ice

Giese 2008; Carton et al. 2000), for the period 1981–2010. All model and observational datasets are interpolated into a 1° latitude–longitude grid and then processed into monthly anomalies by subtracting the long-term mean.

Skill metrics

The ACC, calculated as the spatial correlation coefficient between the MAF forecast and the observations in the offshore area of China (0°–45°N, 105°–135°E) for each target month, are used as the deterministic prediction skill measures. We estimate the prediction skill of the MAF from 1- to 12-month lead times for the 23 CMIP6 models and their MME.

Results

In Wang et al. (2020a), the tropical Indo-Pacific was determined as the initial field of analog criteria. First, we check the prediction skill for the offshore-area-of-China SSTAs using the tropical Indo-Pacific (30°S–30°N, 30°E–80°W) as the initial field of analog criteria (Fig. 1a–c), and then compare the skill of using a reduced range to the western North Pacific (0°–40°N, 90°–150°E) as the

initial field for analog criteria (Fig. 1d–f). The ACC at a 3-month lead is close to 0.6 in the SCS when the reduced range is used (Fig. 1e), which is much greater than the prediction skill using the tropical Indo-Pacific. Although many observational studies have suggested that the western North Pacific SSTA can be influenced by the Indo-Pacific SSTAs (Cao et al. 2013; He et al. 2015; Li and Li 2017; Liu et al. 2014; Tan and Cai 2012), this result shows when the range of the initial field is much larger than the target region the extended regions could induce some disturbances in the MAF prediction method to decrease the prediction skill. Wang et al. (2020a) suggested that SSHAs can provide some information in the subsurface ocean, which is helpful for SSTA prediction in the tropical Indo-Pacific. Here, we compare the prediction skill with and without SSHAs as the predictors (Fig. 1d–i). The results show that SSHAs can improve the prediction skill in the SCS and ECS but decrease the skill in the YBS, which implies that the SSTAs in the SCS and ECS could be connected more closely than those of the YBS to the large-scale ocean dynamics.

In Fig. 1, high prediction skills are mainly located south of 20°N, which may imply a high predictability for the off-shore-area-of-China SSTA from the tropical part of the western North Pacific. We further test a smaller region bounded by (24°–32°N, 122°–128°E), mainly covering the ECS, to evaluate the influence of the initial field on the prediction skill for higher latitude SSTAs in the offshore area of China. As shown in Fig. 2, the ACCs at 1-, 3- and 6-month leads are enhanced over the ECS and YBS relative to those in Fig. 1, but significantly diminished over the other regions. This result suggests that a relatively large range to the initial field cannot only provide more information for the prediction but also bring in more noise, which may improve the total prediction skill for the whole region but worsen the prediction skill in some specific regions. Therefore, more optimization should be performed to find a practical prediction for a specific region. Based on such optimization, in this study, the initial field for prediction over the SCS region (2°–22°N, 105°–120°E) is bounded by (0°–40°N, 90°–150°E), and that over the ECS region is bounded by (24°–32°N, 122°–128°E). Moreover, the prediction skill with only SSTA as the predictor (Fig. 2d–f) is apparently higher than that with SSTA and SSHA as the predictors (Fig. 2a–c), which is consistent with the results related to the ECS and YBS in Fig. 1.

Figure 3a, b shows the SSTA prediction skill over the SCS region from a 1- to 12-month lead time based on 23 CMIP6 models with and without SSHA as the predictor, respectively. The prediction skill shows a large spread among the models, but the MME prediction shows apparently higher skill than any single model.
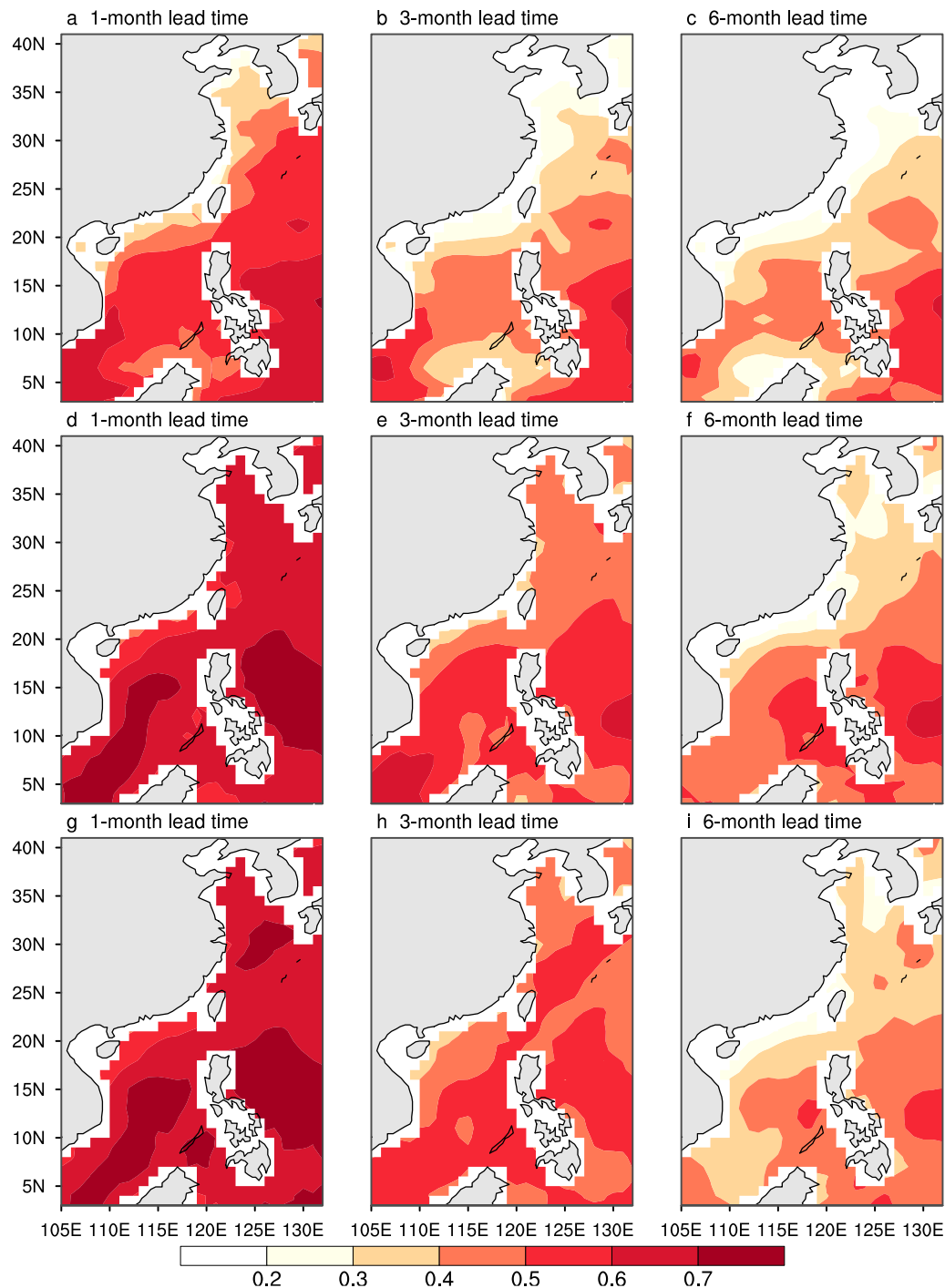
Fig. 1 Prediction skill over the offshore China region measured by the ACC in the MME of the 23 CMIP6 models at 1- (left), 3- (center) and 6-month (right) lead times. **a**–**c** show the initial field of the analog criteria bounded by (30°S–30°N, 30°E–80°W), and **d**–**i** by (0°–40°N, 90°–150°E). The prediction variables are SSTA and SSHA in (**a**–**f**), and SSTA only in (**g**–**i**)

The MME result is consistent with previous MAF predictions and dynamic model predictions in which it was found that an MME prediction can eliminate some noise in individual models and, therefore, enhance the prediction skill (DelSole et al. 2014; Ding et al. 2019; Kirtman et al. 2014). From a 1- to 8-month lead time, the skill of

Fig. 2 As in Fig. 1 but for the initial field of the analog criteria bounded by (24°–32°N, 122°–128°E). The prediction variables are SSTA and SSHA in **a**–**c**, and SSTA only in **d**–**f**
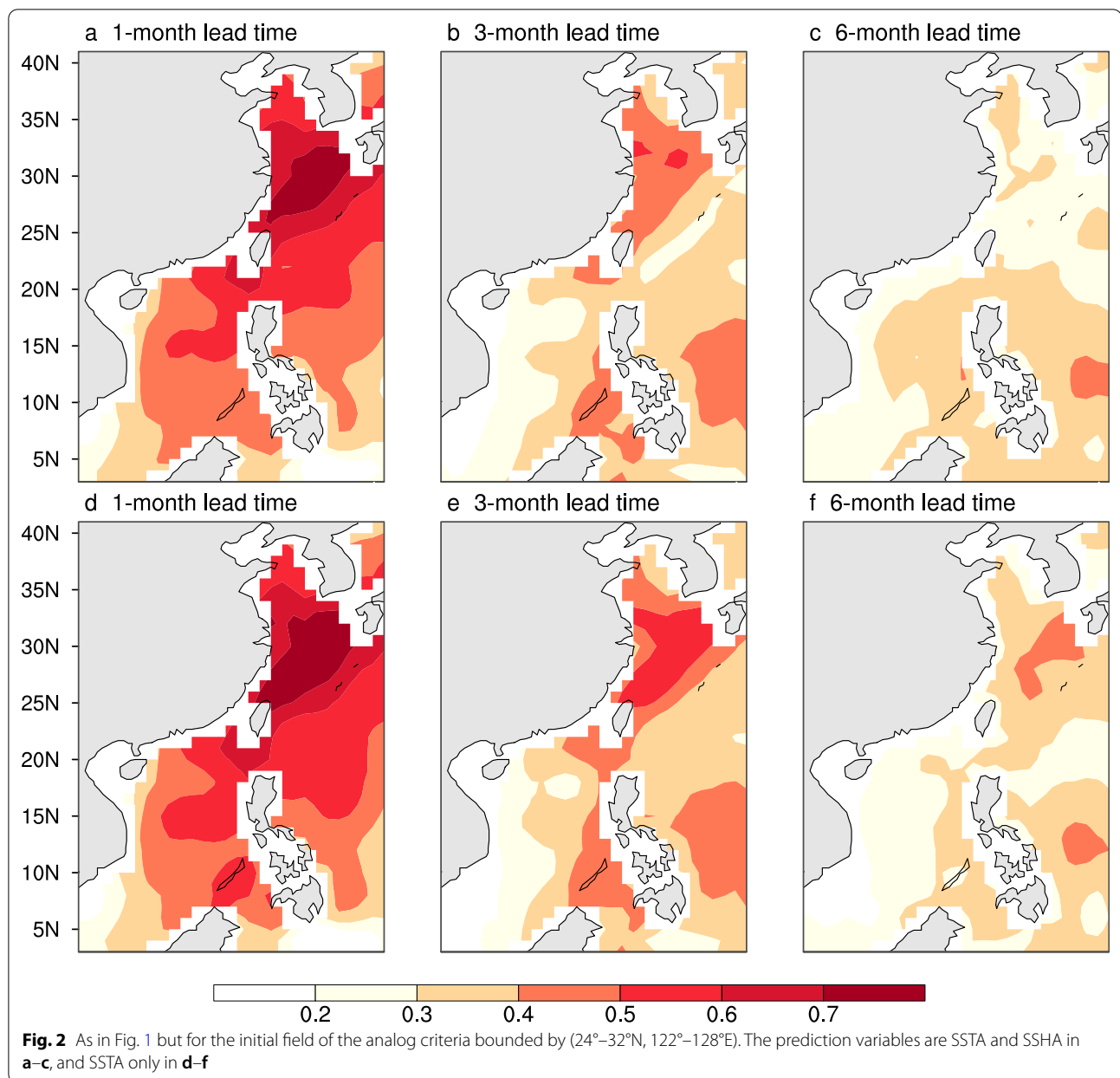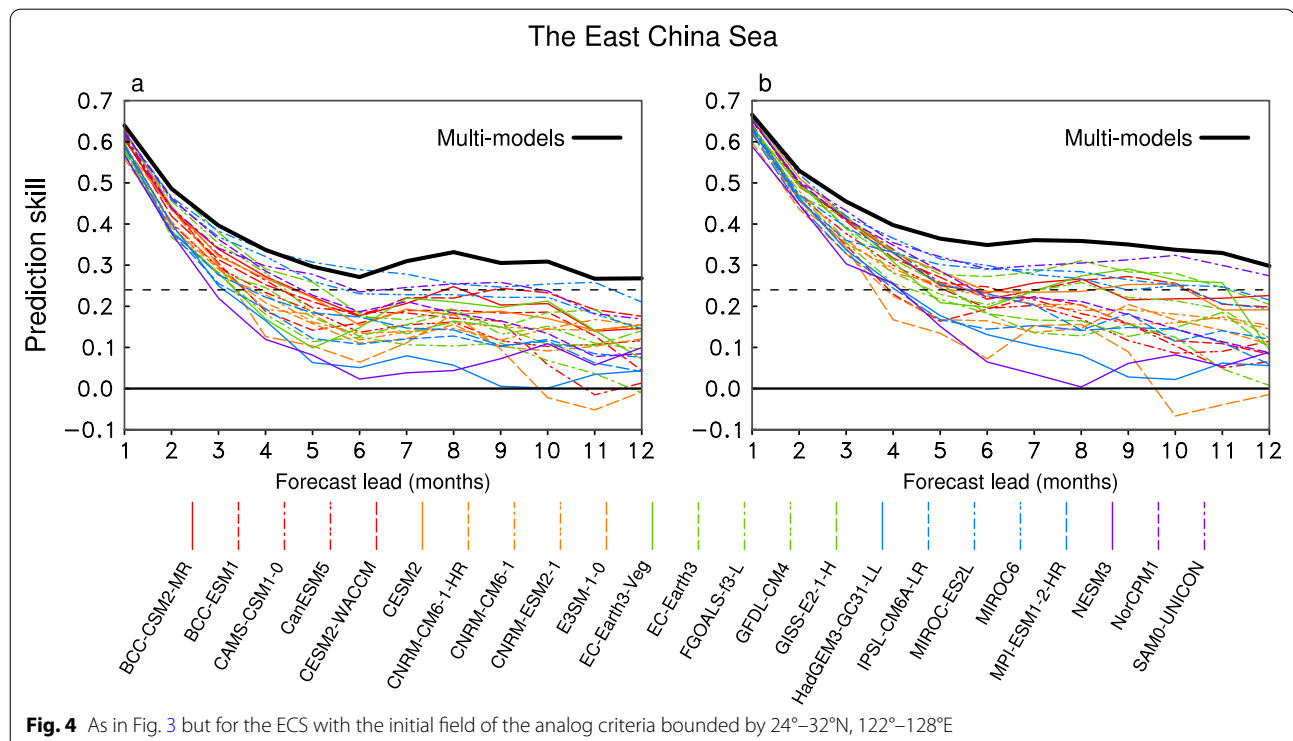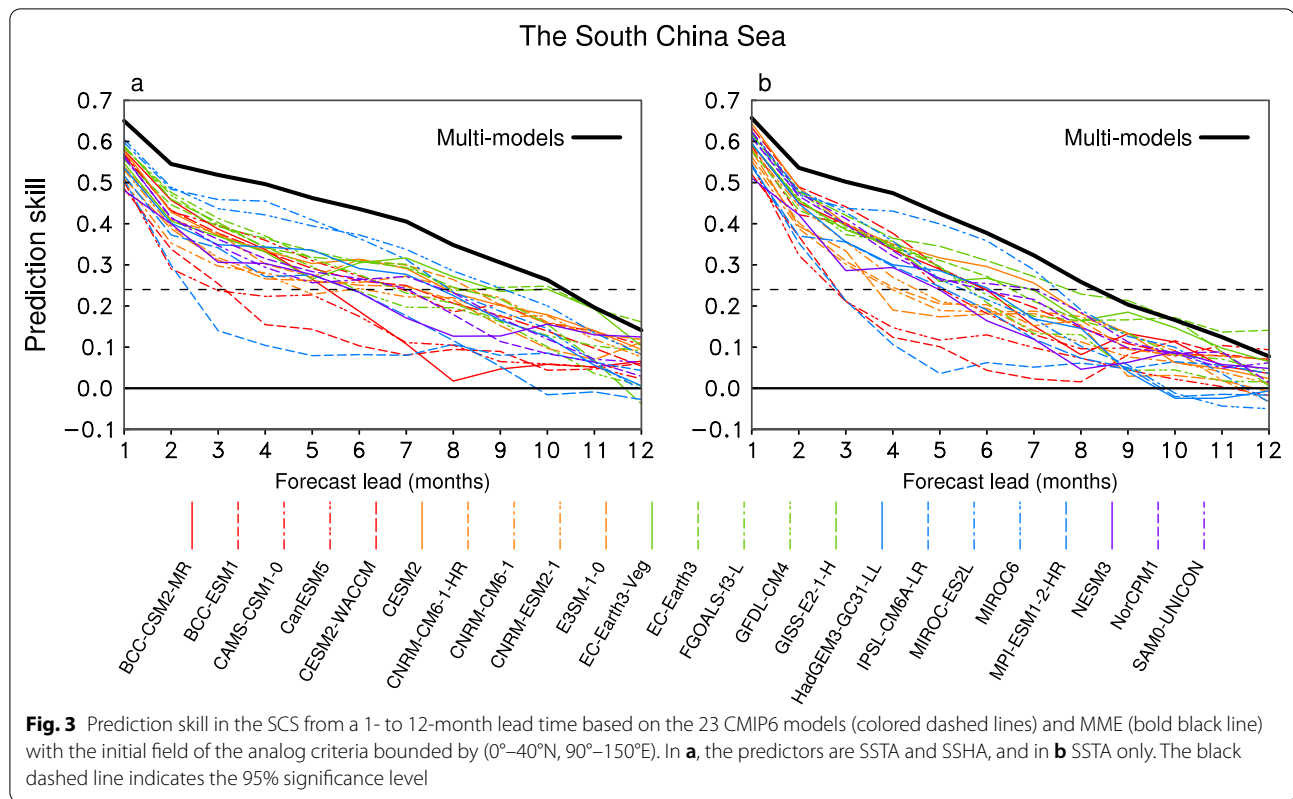
the MME prediction (bold black line in Fig. 3a) is significant at the 95% confidence level and exceeds 0.5 at the 3-month lead. Comparing Fig. 3a and b, we can see that the prediction skill with SSTA and SSHA included in the predictors (Fig. 3a) is higher than that with only SSTA as the predictor (Fig. 3b) in all leading months, especially at a 6- to 12-month lead.

Figure 4 shows the prediction skill of the ECS SSTAs in the MME after optimization of the range of the initial values. The ACC of the MME prediction (bold black line in Fig. 4a) exceeds 0.4 at a 3-month lead. Although this prediction skill of the ECS SSTAs is lower than that

of the SCS SSTAs, this skill is much higher than previous dynamic model predictions. In contrast to the SCS SSTAs, the prediction skill with only SSTA as the predictor (Fig. 4b) in the ECS SSTAs is higher than that with both SSTA and SSHA as the predictors.

In addition, previous studies have suggested that the SSTA tendency (δ SSTA) and ASIA could be potential predictors in the seasonal forecasting of SST over the offshore China region (Deser et al. 2010; Mooley and Munot 1997; Wang et al. 2015a; Wu and Kirtman 2007; Zheng et al. 2014). We further add these factors as predictor variables and choose different combinations of all predictor

Fig. 3 Prediction skill in the SCS from a 1- to 12-month lead time based on the 23 CMIP6 models (colored dashed lines) and MME (bold black line) with the initial field of the analog criteria bounded by (0°–40°N, 90°–150°E). In **a**, the predictors are SSTA and SSHA, and in **b** SSTA only. The black dashed line indicates the 95% significance level

Fig. 4 As in Fig. 3 but for the ECS with the initial field of the analog criteria bounded by 24°–32°N, 122°–128°E

Peng *et al. Geosci. Lett.*   (2021) 8:8

Page 7 of 8

variables (SSTA, SSHA, δ SSTA and ASIA) to improve the prediction skill of the MAF method over the offshore area of China. When the predictors consist of the SSTA and δ SSTA, the spatial pattern of the ACC (not shown) is very close to that in Fig. 1. In the prediction with the predictors consisting of the SSTA and ASIA (only 19 of 23 CMIP6 models support the output of this variable), the total prediction skill can even decrease by more than 0.1 over both the SCS and ECS regions, as compared with the prediction based only on the SSTA.

Conclusions and discussion

In this paper, we apply the MAF method to predict the SSTA over the offshore area of China based on the piControl simulations of 23 CMIP6 models. We evaluated the impact of initial field on the prediction of specific regions from a 1- to 12-month lead time. The MAF method can capture the SSTA evolution over the offshore area of China, with the ACC at the 3-month lead exceeding 0.6 over the SCS region and 0.4 over the ECS region, respectively. The prediction skill of the 23 CMIP6 models shows large intermodel spread. The MME of all models can greatly improve the prediction skill relative to any single model prediction.

The optimal initial field of the analog criteria should be decided by the target region. For the prediction of the tropical oceans, it is reasonable to choose a tropical area as the initial field (Chen et al. 2020; Ding et al. 2018, 2019; Wang et al. 2020a). Therefore, the choice of the western North Pacific region as the initial field in this study can greatly improve the prediction skill of the SSTA over the offshore area of China from 0.35 to 0.6. Meanwhile, the sensitivity of the prediction skill to the choice of initial field is also tested. The result suggests that a larger area (0°−40°N, 90°−150°E) over the western North Pacific is more suitable for the SCS region, and a smaller core area (24°−32°N, 122°−128°E) for the ECS region. The prediction skill of the predictors, SSTA and SSHA, are tested for different subregions of the offshore China region. The SSHA can apparently improve the prediction skill for the SCS SSTAs but not for the ECS SSTAs.

We also test some other potential predictors for the prediction of the offshore China SSTAs, such as the SSTA tendency and ASIA. Although some previous observational studies have suggested that these factors could influence the SSTAs in the offshore China region, we find no apparent improvement in the prediction skill when these factors are added as predictors in the MAF method, possibly due to the weaknesses of the CMIP6 models in simulating the impact of these factors on the offshore China SSTAs. Moreover, due to the limitation of the spatial resolutions of the CMIP6 models in the YBS, the MAF method cannot provide a competitive prediction for the YBS SSTAs, although the ACC of the prediction skill for the YBS is somewhat improved relative to previous dynamic model predictions (Ma and Wang 2014; Wang et al. 2013; Wang 2015b; Zhang et al. 2018).

Abbreviations
MAF: Model-based analog forecasting; ECS: East China Sea; YBS: Yellow Sea and Bohai Sea; SCS: South China Sea; SST: Sea surface temperature; SSTA: Sea surface temperature anomaly; CMIP: Coupled Model Intercomparison Project; CMIP6: Phase 6 of the Coupled Model Intercomparison Project; piControl: Pre-industrial control; RMS: Root-mean-square; MME: Multi-model ensemble mean; SSHA: Sea surface height anomaly; δ SSTA: Sea surface temperature anomaly tendency; ASIA: Arctic sea-ice anomaly; HadISST: Met Office Hadley Centre's Sea Ice and Sea Surface Temperature dataset; SODA: Simple Ocean Data Assimilation; ACC: Anomaly correlation coefficient.

Authors' contributions
PH and QC conceived and designed the study, WP performed the prediction, and WP, SZ and PH wrote the paper. All authors discussed and commented on the paper. All authors read and approved the final manuscript.

Availability of data and materials
The HadISST dataset can be obtained from https://climatedataguide.ucar.edu/climate-data/sst-data-hadisst-v11; the SODA dataset can be obtained from https://climatedataguide.ucar.edu/climate-data/soda-simple-ocean-data-assimilation; CMIP6 datasets can be obtained from https://esgf-node.llnl.gov/projects/cmip6/.

Declaration

Competing interests
The authors declare that they have no competing interests.

Author details
[1] Chengdu University of Information Technology, Chengdu, China. [2] Center for Monsoon System Research, Institute of Atmospheric Physics, Chinese Academy of Sciences, Beijing, China. [3] State Key Laboratory of Numerical Modeling for Atmospheric Sciences and Geophysical Fluid Dynamics, Institute of Atmospheric Physics, Chinese Academy of Sciences, Beijing, China.

References
Barnston AG, Tippett MK, Ranganathan M, L'Heureux ML (2019) Deterministic skill of ENSO predictions from the North American Multimodel Ensemble. Clim Dyn 53:7215–7234. https://doi.org/10.1007/s00382-017-3603-3

Cai R, Chen J, Huang R (2006) The response of marine environment in the offshore area of China and its adjacent ocean to recent global climate change. Chin J Atmos Sci 30:1019–1033 (**in Chinese**)

Cai R, Chen J, Tan H (2011) Variations of the sea surface temperature in the offshore area of China and their relationship with the East Asian monsoon under the global warming. Clim Environ Res 16:95–104 (**in Chinese**)

Cao J, Lu R, Hu J, Wang H (2013) Spring Indian Ocean-western Pacific SST contrast and the East Asian summer rainfall anomaly. Adv Atmos Sci 30:1560–1568. https://doi.org/10.1007/s00376-013-2298-6

Carton JA, Giese BS (2008) A reanalysis of ocean climate using Simple Ocean Data Assimilation (SODA). Mon Weather Rev 136:2999–3017. https://doi.org/10.1175/2007mwr1978.1

Peng *et al. Geosci. Lett.* (2021) 8:8

Page 8 of 8

Carton JA, Chepurin G, Cao X (2000) A simple ocean data assimilation analysis of the global upper ocean 1950–95. Part I Methodol J Phys Oceanogr 30:294–309. https://doi.org/10.1175/1520-0485(2000)030%3C0294:ASODAA%3E2.0.CO;2

Chen Z, Xu D, Dai G, Zhang Y, Zhong S, Huang Y (2020) Technical scheme and operational system of tropical high-resolution model (TRAMS-V3.0). J Trop Meteorol 36:444–454. https://doi.org/10.16032/j.issn.1004-4965.2020.041 (**in Chinese**)

DelSole T, Nattala J, Tippett MK (2014) Skill improvement from increased ensemble size and model diversity. Geophys Res Lett 41:7331–7342. https://doi.org/10.1002/2014GL060133

Deser C, Tomas R, Alexander M, Lawrence D (2010) The seasonal atmospheric response to projected Arctic sea ice loss in the late twenty-first century. J Clim 23:333–351. https://doi.org/10.1175/2009jcli3053.1

Ding H, Newman M, Alexander MA, Wittenberg AT (2018) Skillful climate forecasts of the tropical Indo-Pacific ocean using model-analogs. J Clim 31:5437–5459. https://doi.org/10.1175/jcli-d-17-0661.1

Ding H, Newman M, Alexander MA, Wittenberg AT (2019) Diagnosing secular variations in retrospective ENSO seasonal forecast skill using CMIP5 model-analogs. Geophys Res Lett 46:1721–1730. https://doi.org/10.1029/2018gl080598

Eyring V, Bony S, Meehl GA, Senior CA, Stevens B, Stouffer RJ, Taylor KE (2016) Overview of the Coupled Model Intercomparison Project Phase 6 (CMIP6) experimental design and organization. Geosci Model Dev 9:1937–1958. https://doi.org/10.5194/gmd-9-1937-2016

Gong Z, Li S, Hu P, Shen B, Feng G (2016) Dynamic-analogue correction of the decadal change of East Asian summer precipitation in the late 1990s. J Meteorol Res 30:341–355. https://doi.org/10.1007/s13351-016-5220-1

He C, Zhou T, Wu B (2015) The key oceanic regions responsible for the interannual variability of the western North Pacific subtropical high and associated mechanisms. J Meteorol Res 29:562–575. https://doi.org/10.1007/s13351-015-5037-3

Keenlyside N, Latif M, Botzet M, Jungclaus J, Schulzweida U (2016) A coupled method for initializing El Niño Southern Oscillation forecasts using sea surface temperature. Tellus, Ser A Dyn Meteorol Oceanogr 57:340–356. https://doi.org/10.3402/tellusa.v57i3.14661

Kirtman BP, Min D, Infanti JM, Iii JLK, Paolino DA, Zhang Q, Dool HVD, Saha S, Mendez MP, Becker E, Peng P, Tripp P, Huang J, Dewitt DG, Tippett MK, Barnston AG, Li S, Rosati A, Schubert SD, Rienecke M, Suarez M, Li ZE, Marshak J, Lim Y-K, Tribbia J, Pegion K, Merryfield WJ, Denis B, Wood EF (2014) The North American Multimodel Ensemble: phase-1 Seasonal-to-Interannual Prediction; phase-2 toward developing Intraseasonal Prediction. Bull Am Meteor Soc 95:585–601. https://doi.org/10.1175/bams-d-12-00050.1

Li X, Li C (2017) The tropical Pacific-Indian Ocean associated mode simulated by LICOM2.0. Adv Atmos Sci 34:1426–1436. https://doi.org/10.1007/s00376-017-6176-5

Li W, Zhang P, Li Q, Wang L, Liu Y, Shi X, Zhang Z (2005) Research and operational applicationof dynamical climate model prediction system. Chin J Appl Meteor 16:1–11. https://doi.org/10.3969/j.issn.1001-7313.2005.z1.001 (**in Chinese**)

Lin C, Ning X, Su J, Lin Y, Xu B (2005) Environmental changes and the responses of the ecosystems of the Yellow Sea during 1976–2000. J Mar Syst 55:223–234. https://doi.org/10.1016/j.jmarsys.2004.08.001

Liu L, Du Y, Qu X, Xie S, Zheng X, Huang G, Hu K (2014) Interdecadal variations in ENSO influences on northwest Pacific-East Asian early summertime climate simulated in CMIP5 models. J Clim 27:5982–5998. https://doi.org/10.1175/jcli-d-13-00268.1

Liu N, Wang H, Ling T, Zu Z (2018) Review and prospect of global operational ocean forecasting. Adv Earth Sci 33:131–140. https://doi.org/10.11867/j.issn.1001-8166.2018.02.0131 (**in Chinese**)

Ma J, Wang H (2014) Design and testing of a global climate prediction system based on a coupled climate model. Sci China-Earth Sci 57:2417–2427. https://doi.org/10.1007/s11430-014-4875-7 (**in Chinese**)

Merryfield WJ, Lee W-S, Boer GJ, Kharin VV, Scinocca JF, Flato GM, Fyfe JC, Ajayamohan RS, Tang Y, Polavarapu S (2013) The Canadian seasonal to interannual prediction system. Part I: models and initialization. Mon Weather Rev 141:2910–2945. https://doi.org/10.1175/mwr-d-12-00216.1

Mooley DA, Munot AA (1997) Relationships between Indian summer monsoon and Pacific SST/SOI tendency from winter to spring and their stability. Theor Appl Climatol 56:187–197

Qi Q, Cai R (2019) Analysis on climate characteristics of sea surface temperature extremes in coastal China seas. Acta Oceanol Sin 41:36–51. https://doi.org/10.3969/j.issn.0253—4193.2019.07.004 (**in Chinese**)

Rayner NA, Parker DE, Horton EB, Folland CK, Alexander LV, Rowell DP (2003) Global analyses of sea surface temperature, sea ice, and night marine air temperature since the late nineteenth century. J Geophys Res 108:1–20. https://doi.org/10.1029/2002jd002670

Ren S, Wang H, Liu N (2015) Review of ocean front in Chinese marginal seas and frontal forecasting. Adv Earth Sci 30:552–563. https://doi.org/10.11867/j.issn.1001-8166.2015.05.0552

Singh D, Kumar A (2020) Analog ensemble (AE) systems for real time quantitative precipitation forecasts (QPFs) for different forecast lead times at local scale over the north-west Himalaya (NWH), India. Meteorol Atmos Phys. https://doi.org/10.1007/s00703-020-00763-0

Song C, Zhang S, Jiang H, Wang H, Wang D, Huang Y (2016) Evaluation and projection of SST in the China seas from CMIP5. Acta Oceanol Sin 38:1–11 (**in Chinese**)

Tan H, Cai R (2012) Possible impact of tropical El Niño Modoki on SST of China offshore and its adjacent waters. J Trop Meteorol 28:897–904. https://doi.org/10.3969/j.issn.1004-4965.2012.06.011 (**in Chinese**)

Tan H, Cai R, Huang R (2016) Enhanced responses of sea surface temperature over offshore China to global warming and hiatus. Progressus Inquisitiones de Mutatione Climatis 12:500–507. https://doi.org/10.12006/j.issn.1673-1719.2016.38 (**in Chinese**)

Toth Z (1987) Long-range weather forecasting using an analog approach. J Clim 2:594–607

Van den Dool HM (1989) A new look at weather forecasting through analogues. Mon Weather Rev 117:2230–2247. https://doi.org/10.1175/1520-0493(1989)117%3c2230:anlawf%3e2.0.co;2

Wang B, Kang I-S, Lee J-Y (2004) Ensemble simulations of Asian-Australian monsoon variability by 11 AGCMs*. J Clim 17:803–818. https://doi.org/10.1175/1520-0442(2004)017%3C0803:ESOAMV%3E2.0.CO;2

Wang Q, Zhang L, Guan J (2013) Monthly dynamical extended-range ensemble forecasts with different SST forcing. Clim Environ Res 18:517–523. https://doi.org/10.3878/j.issn.1006-9585.2013.12162 (**in Chinese**)

Wang H, Chen H, Liu J (2015a) Arctic sea ice decline intensified haze pollution in eastern China. Atmos Oceanic Sci Lett 8:1–9. https://doi.org/10.3878/AOSL20140081

Wang X, Zheng Z, Feng G, Wang K, Shen Q (2015b) Summer prediction of sea surface temperatures in key areas in BCC_CSM model. Chin J Atmos Sci 39:271–288. https://doi.org/10.3878/j.issn.1006-9895.1408.13329 (**in Chinese**)

Wang Y, Zhang Z, Huang P (2020a) An improved model-based analogue forecasting for the prediction of the tropical Indo-Pacific Sea surface temperature in a coupled climate model. Int J Climatol 40:6346–6360. https://doi.org/10.1002/joc.6584

Wang Z, Li Y, Wang X (2020b) Development of forecast guidance product for sea temperature of basic forecast units in the Chinese coastal waters. Mar Forecasts 37:59–65. https://doi.org/10.11737/j.issn.1003-0239.2020.04.007 (**in Chinese**)

Wei K, Ouyang C, Duan H, Li Y, Chen M, Ma J, An H, Zhou S (2020) Reflections on the Catastrophic 2020 Yangtze river basin flooding in Southern China. Innovation. https://doi.org/10.1016/j.xinn.2020.100038

Wu R, Kirtman BP (2007) Regimes of seasonal air–sea interaction and implications for performance of forced simulations. Clim Dyn 29:393–410. https://doi.org/10.1007/s00382-007-0246-9

Zhang S, Song C, Wang H, Jiang H, Du L (2018) Evaluation of the hindcasting main SSTA modes of the global key regions based on the CESM forecasting system. Acta Oceanol Sin 40:18–30. https://doi.org/10.3969/j.issn.0253-4193.2018.09.002 (**in Chinese**)

Zheng J, Ren B, Li G, Yang C (2014) Seasonal dependence of local air-sea interaction over the tropical western Pacific warm pool. J Trop Meteorol 20:360–367. https://doi.org/10.16555/j.1006-8775.2014.04.009

Publisher's Note